AIP | APL Materials

NOW INDEXED IN THOMSON REUTERS DATABASES

Impact of the organic halide salt on final perovskite composition for photovoltaic applications

David T. Moore, Hiroaki Sai, Kwan Wee Tan, Lara A. Estroff, and Ulrich Wiesner

Citation: APL Materials **2**, 081802 (2014); doi: 10.1063/1.4886275
View online: http://dx.doi.org/10.1063/1.4886275
View Table of Contents: http://scitation.aip.org/content/aip/journal/aplmater/2/8?ver=pdfcov
Published by the AIP Publishing

APL MATERIALS **2**, 081802 (2014)

Impact of the organic halide salt on final perovskite composition for photovoltaic applications

David T. Moore, Hiroaki Sai, Kwan Wee Tan, Lara A. Estroff, and Ulrich Wiesner[a]
Department of Materials Science and Engineering, Cornell University, Ithaca, New York 14853, USA

(Received 2 May 2014; accepted 20 June 2014; published online 7 July 2014)

The methylammonium lead halide perovskites have shown significant promise as a low-cost, second generation, photovoltaic material. Despite recent advances, however, there are still a number of fundamental aspects of their formation as well as their physical and electronic behavior that are not well understood. In this letter we explore the mechanism by which these materials crystallize by testing the outcome of each of the reagent halide salts. We find that components of both salts, lead halide and methylammonium halide, are relatively mobile and can be readily exchanged during the crystallization process when the reaction is carried out in solution or in the solid state. We exploit this fact by showing that the perovskite structure is formed even when the lead salt's anion is a non-halide, leading to lower annealing temperature and time requirements for film formation. Studies into these behaviors may ultimately lead to improved processing conditions for photovoltaic films. [http://dx.doi.org/10.1063/1.4886275]

For many crystalline semiconductors, the ability to grow large, oriented grains is essential for high performance. This ability is enabled, in part, by a fundamental understanding of the mechanisms by which the crystal forms. The methylammonium lead halide perovskites ($MAPbX_3$, where $MA = NH_3CH_3^+$, $X = I^-$ or Cl^-) have recently shown great promise as a class of photovoltaic materials that can yield high efficiency devices using low cost processing methods.[1–21] Power conversion efficiencies of these devices are enhanced by the control of perovskite film coverage and crystallinity.[12,17,19–24] We have previously reported three stages of structural evolution in the perovskite formation via a one-step solution-processing route: an unidentified crystalline precursor structure, the perovskite structure, and decomposition products.[23] Specifically the transition from the precursor structure to the perovskite structure is intriguing since it indicates a solid-state transformation. In this letter we show that the perovskite structure forms via complete dissociation and rearrangement of all reagent halide salts under both solution and solid state conditions. Based on this knowledge we explore alternative synthetic routes with the ultimate goal of finding more favorable processing conditions for the formation of the desired perovskite structure.

The formation of thin films of $MAPbX_3$ can be accomplished through several processing routes as shown schematically in Figure 1. Various groups have reported a one-step deposition method (Fig. 1(a)) that consists of mixing a lead halide salt (PbX_2, $X = I^-$, Cl^-) and a methylammonium halide salt (MAX, $X = I^-$, Cl^-) in a common solvent and depositing the solution on a substrate. Upon thermal annealing, the solvent is removed and the perovskite structure is formed.[3,4,9,14,15,17,20,22–28] A common pathway for this type of crystallization from solution is by the rearrangement of constituent ions; however, for solid-state transitions there are other viable pathways to consider, such as the topotactic transformation of one or more of the constituent salts.[29–34] Determining the pathway by

[a]Author to whom correspondence should be addressed. Electronic mail: ubw1@cornell.edu.

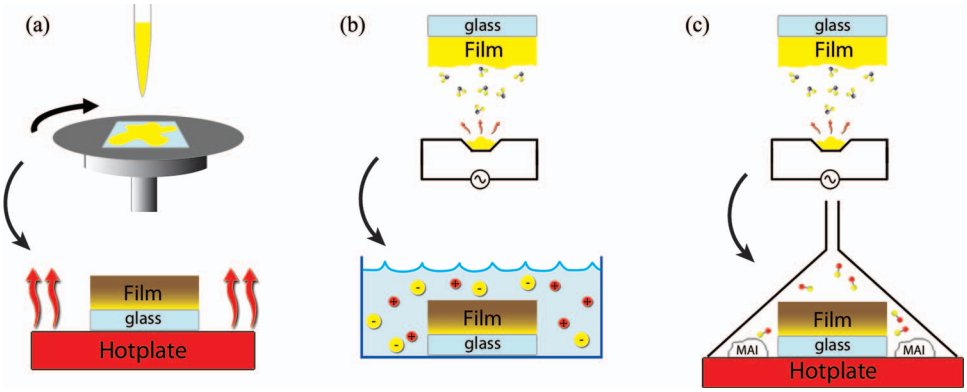

FIG. 1. Schematic of perovskite thin film processing pathways: (a) One-step solution deposition from both halide salts in a common solvent via spin coating followed by thermal annealing. (b) Two-step process by soaking a thermally evaporated film of lead halide in a solution of MA halide dissolved in an anti-solvent for the perovskite. (c) Two-step process using a thermally evaporated film of lead halide followed by sublimation of the MA halide salt.

TABLE I. Experimental parameters of $MAPbX_3$ perovskite formation studies.

Sample label	Lead halide[a]	[MAI] (mM)[b]	[MACl] (mM)[b]	Perovskite formed[c]
I-120	PbI_2	120	0	$MAPbI_n$
C-120	$PbCl_2$	120	0	$MAPbI_n$
I-80	PbI_2	80	40	$MAPbI_n$
C-80	$PbCl_2$	80	40	$MAPbI_n$
I-40	PbI_2	40	80	$MAPbCl_n$
C-40	$PbCl_2$	40	80	$MAPbCl_n$
I-0	PbI_2	0	120	$MAPbCl_n$
C-0	$PbCl_2$	0	120	$MAPbCl_n$

[a]The 1 μm thick lead salt films were thermally evaporated.
[b]MA halide solutions were prepared in isopropyl alcohol.
[c]$MAPbX_n$ denotes $MAPbX_{3-m}Y_m$ where $m \ll 1$.

which the perovskite forms has implications both in terms of potential processing conditions, as well as providing a means by which the role of other components, such as spectator species, can be explored.

In order to decouple the disposition of the reagent salts, we adopted a two-step process,[12] in which we deposited the lead salt by thermal evaporation followed by soaking the films in a solution of methylammonium halides dissolved in isopropanol (Fig. 1(b)). Due to the minimal solubility of lead halides in isopropanol, this processing route has the lead halide in the solid state during the crystallization; it is important to note the solubility of the resulting perovskite is negligible in isopropyl alcohol (IPA) but quite high in water mandating the use of a water free environment for this experimental path. We varied the deposited lead halide species and the molar ratios of the methylammonium halides (MAI and MACl) as summarized in Table I. We note that given the lead salt film thickness and the volume of solution used, there is an approximately 3000-fold excess of methylammonium halide in the solution compared to the lead halide on the substrate, leaving lead as the only limiting reagent in the reaction. Preliminary experiments on thin lead halide films (25–100 nm) showed that delamination from the substrate occurred prior to complete formation of the perovskite. To mitigate this effect, 1 μm thick lead halide films were used, thereby simultaneously avoiding delamination and ensuring thick enough perovskite layers for characterization. In order to maintain the structure, as formed in the thin film, without excluding structural elements due to texturing, we performed grazing incidence wide-angle X-ray scattering (GIWAXS) directly on those films. Figure 2 shows the azimuthally integrated intensity plots of the resulting two-dimensional (2D) data sets. Previous studies, including energy-dispersive X-ray

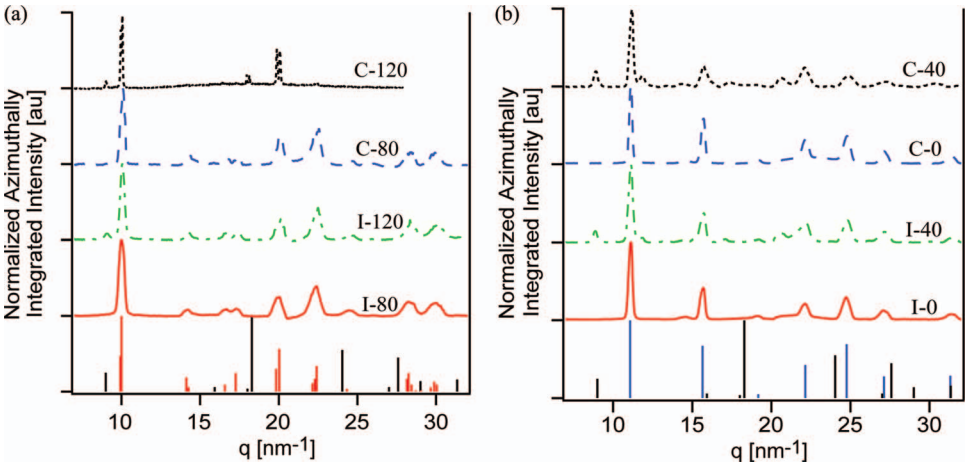

FIG. 2. Azimuthally integrated GIWAXS data, for evaporated lead halide films soaked in various methylammonium halide solutions, plotted against the scattering vector q, where $q = 4\pi \sin\theta/\lambda$. (a) Films in which MAI was in higher concentration and (b) films in which MACl was in higher concentration. Stick markers at the bottom of the plots indicate calculated peak locations for the tetragonal iodide perovskite (red),[35] the cubic chloride perovskite (blue),[36] and lead iodide (black).[37] Note: Sample C-120 was damaged prior to GIWAXS collection; the data shown are a 2-theta scan of an equivalently prepared film.

spectroscopy (EDX)[25] and X-ray photoelectron spectroscopy (XPS),[15] have shown that Cl can only be incorporated into the iodide structure at very low concentrations; additionally, for the mixed halide systems that do form a continuous solid solution (I/Br and Cl/Br)[3,35] there is a systematic shift in both the lattice parameter and the optical band gap. Given these facts we used the x-ray patterns and/or absorption data to determine the primary structure formed; although this does not determine the purity of the structure, small inclusions of the secondary halide do not impact the assessment of the extent of the dissociation/rearrangement of the reagent salts. As summarized in Table I, the scattering patterns reveal that the final perovskite structure contains the halide species dominant in the solution, regardless of the starting lead halide film. This result suggests that the lead halide needs to dissociate and exchange freely with the methylammonium halide ions during the process of the perovskite formation. Based on the observed behavior of ion rearrangement, as well as results of an earlier study in which we reported the existence of a structurally unidentified precursor phase prior to the perovskite,[23] it is clear that the pathway of the system to the final perovskite structure is rather complex and deserves further study.

We note that the crystallization times and crystal morphologies vary with the lead halide source. For lead chloride films the soaking time required to obtain the perovskite was 4 h, compared to 2 h for the lead iodide films. SEM and 2D GIWAXS data (see the supplementary material)[38] show that lead iodide films lead to perovskite structures with much smaller crystals, better coverage, and a higher degree of crystallographic orientation. The most highly textured films, based on the GIWAXS data, are samples I-120 and I-80, both of which start with PbI_2 and transform to $MAPbI_3$ (Figs. S1(a) and S1(c) of the supplementary material).[38] From the SEM image (Fig. S2(a)) of the supplementary material[38] of I-80 this texture appears to be the result of the homogeneity of both the size and shape of the crystallites, which leads to better packing and orientational order of the individual grains. The slower growth of the corresponding $PbCl_2$ sample, C-80, leads to crystals that are larger and more polydisperse in both size and shape. The SEM image (Fig. S2(b) of the supplementary material)[38] shows sparse coverage and a random orientation of the individual crystals, causing a less textured scattering pattern (Fig. S1(d) of the supplementary material).[38]

We next turned our attention to the outcome of the MA salt and the question of whether the individual ions of the MA halide stay associated or not. The reverse version of the above soaking experiment, i.e., soaking solid state MAX films in PbX_2 solutions, is impractical as the lead halides are only appreciably soluble in solvents that will also solvate the perovskite. However, we can explore the disposition of the MA salt in the solid state by using a two-step sublimation process similar to that reported by Chen *et al.*[19] in which the lead salt is deposited first and the MA salt

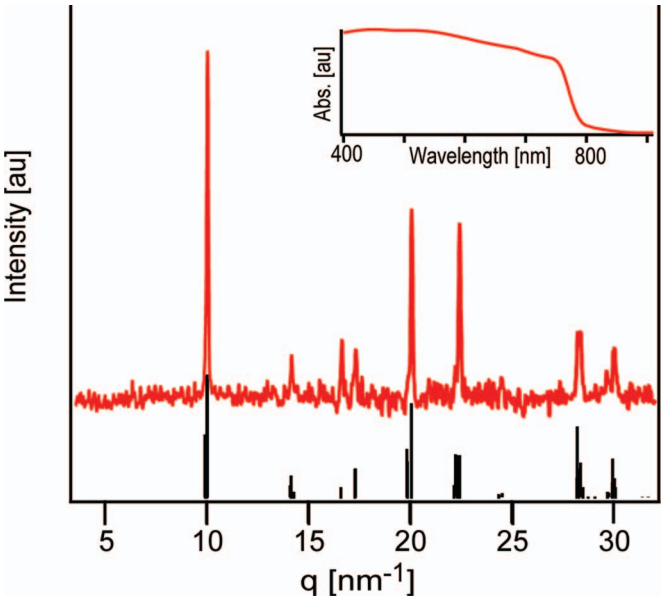

FIG. 3. XRD pattern (red) of evaporated $PbCl_2$ thin film transformed by sublimation of MAI at 150 °C; stick markers (black) indicate expected peak positions for the iodide perovskite. Inset shows the absorbance spectrum of the same film.

introduced by sublimation. For many ionic salts, specifically ammonium salts, it has been shown that sublimation at lower temperatures produces molecular units in the vapor phase as opposed to dissociated ions.[39,40] We therefore assume that the sublimed species is, e.g., molecular MAI which then condenses onto the lead salt film followed by the crystallization of the perovskite. This process is a solid state reaction with no background solvent present. Thin films (∼50 nm) of lead chloride were first evaporated onto glass substrates. The films were placed on a hotplate at 150 °C, together with a small volume of MAI salt and covered with a funnel to allow for saturation with MAI vapor (see Fig. 1(c)). The films began to turn brown at the edges in ∼1 h and were completely brown after 7 h. Comparison of the XRD spectrum (Fig. 3) to the known peak positions for $MAPbI_3$ confirms that the iodide perovskite structure was formed. The inset of Figure 3 presents the absorption spectrum of the final film, exhibiting a band gap also consistent with the iodide perovskite.[2,3] Given that the lead halide was $PbCl_2$, the stoichiometry dictates that the MAI must have dissociated to form the resulting perovskite. The results therefore suggest that all ions dissociate, not only when the reaction is performed in solution, but also when both salts are present in the solid state, with no solvent present.

The crystallization pathway reported here raises several interesting questions. These questions include, among others: Are there possible routes to templating the crystal growth via the individual, constituent ions? Does this pathway help elucidate the role of spectator species in mediating the dissociation of the reagents? How sensitive is the formation of the final perovskite to the source of the constituent ions? We explore one of these ideas as further validation of our findings and to demonstrate the application of these results to finding alternative processing pathways. If the lead cation loses all association with its corresponding anions during the crystallization process, then the crystallization should be insensitive to the lead source. To verify the insensitivity to the lead counter-ions and to test the impact of the lead source on processing conditions, we prepared a film using lead nitrate, $Pb(NO_3)_2$, a non-halide lead source. A 40 wt.% solution of $Pb(NO_3)_2$ and MAI in a 1:3 stoichiometric ratio was prepared in *N*,*N*-dimethylformamide (DMF) and spin-cast onto a glass substrate at 2500 rpm for 45 seconds. After spin-casting, the substrate was placed on a hotplate and ramped from room temperature to 100 °C at 1 °C/min. These are the same conditions that we have previously reported for the mixed halide of $PbCl_2$:MAI in DMF,[22,23] except that in the mixed halide system the total post-deposition treatment consisted of the ramp to 100 °C followed by

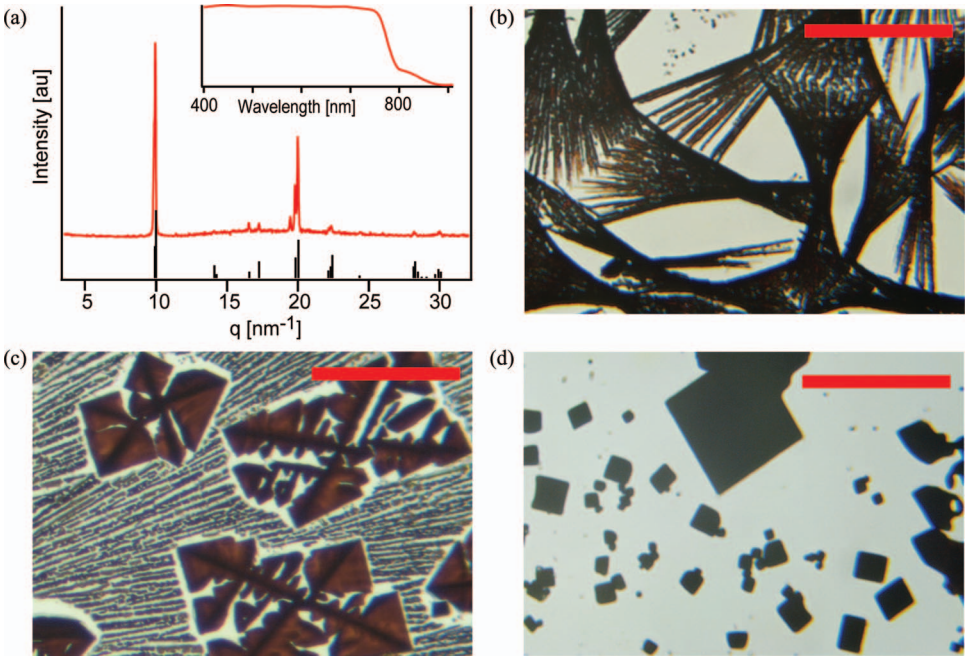

FIG. 4. Characterization of perovskite films with $Pb(NO_3)_2$ as the Pb source. (a) XRD pattern and absorbance spectrum (inset) of the spin coated film. Vertical markers (black) indicate expected peak positions of the iodide perovskite. (b)–(d) Optical micrographs of spray coated films. Scale bars in all images are 50 μm.

45 min of annealing at that temperature. In our tests with $Pb(NO_3)_2$-based solutions, the films turned brown at ~20 min into the temperature ramp, corresponding to a temperature of only 45 °C.

Figure 4 shows the XRD pattern, absorption data, and optical images of perovskite films with $Pb(NO_3)_2$ as the lead source. The x-ray diffraction and absorbance data (Fig. 4(a)) confirm that $MAPbI_3$ is formed. The faster formation of the perovskite at lower temperatures is likely the result of the spectator species, $MANO_3$, the excess component that exists as a result of the non-stoichiometric reagents in solution. In the mixed halide system used by several groups,[15,17,24,25,41] with $PbCl_2$:MAI in a 1:3 ratio, the excess component is MACl (m.p. ≈ 230 °C), which is less volatile then $MANO_3$ (m.p. ≈ 110 °C). Although the relationship between volatility and lower annealing temperatures is unclear, it does provide potential alternate processing paths, such as spray coating. The optical images in Figs. 4(b)–4(d) were taken from spray coated films prepared in identical ways at different times. These micrographs reveal two important features: (1) a high sensitivity of the resulting film morphology to subtle changes in the growth conditions like environmental humidity, which was not controlled in these experiments; (2) the various morphologies that can be achieved, including spherulites (Fig. 4(b)), dendrites (Fig. 4(c)), and large faceted crystals (Fig. 4(d)). Because the annealing temperature was well below that used for films made from $PbCl_2$ (in which the excess salt has been reported to be removed by sublimation during annealing)[20] we checked to ensure that the excess salt ($MANO_3$) was completely removed. To that end additional films were made and the presence of NO_3 probed by FTIR, after which the films were soaked for 3 min in IPA, then rinsed thoroughly with IPA, and probed again. The resulting spectra (Figure S3 of the supplementary materials)[38] show that NO_3 is still present in the films after annealing but that it is completely removed by washing. These results suggest that crystallization of the perovskite can occur in the presence of excess organic salt.

In conclusion, we have probed the disposition of both reagent salts used in the processing of $MAPbX_3$ thin films and showed that the crystallization occurs via rearrangement of all constituent ions, irrespective of whether the reaction is performed in solution or in the solid state. We have noted several implications of this crystallization mechanism and demonstrated that one of those, the choice of the lead counter-ion, can be exploited to effect the annealing time and temperature

necessary to form the final product. The results suggest that fundamental materials research as shown here, targeted at understanding the crystallization mechanisms, may ultimately help elucidate improved processing conditions leading to thin films of perovskites with optimized crystal size and orientation, which, in turn, may give rise to enhanced opto-electronic properties.

The authors acknowledge financial support from the National Science Foundation through Materials World Network grants (DMR-1008125 and DMR 1210304). K.W.T. gratefully acknowledges the Singapore Energy Innovation Programme Office for a National Research Foundation graduate fellowship. This work made use of the research facilities of the Cornell Center for Materials Research (CCMR) with support from the NSF Materials Research Science and Engineering Centers (MRSEC) program (DMR-1120296), Cornell High Energy Synchrotron Source (CHESS) which is supported by the NSF and the NIH/National Institute of General Medical Sciences under NSF Award No. DMR-0936384, and the KAUST-Cornell Center for Energy and Sustainability supported by Award No. KUS-C1-018-02, made by King Abdullah University of Science and Technology (KAUST). The authors gratefully acknowledge Trent Scott of Cornell University for his experimental assistance.

[1] M. M. Lee, J. Teuscher, T. Miyasaka, T. N. Murakami, and H. J. Snaith, Science **338**, 643 (2012).
[2] H.-S. Kim, C.-R. Lee, J.-H. Im, K.-B. Lee, T. Moehl, A. Marchioro, S.-J. Moon, R. Humphry-Baker, J.-H. Yum, J. E. Moser, M. Grätzel, and N.-G. Park, Sci. Rep. **2**, 591 (2012).
[3] J. H. Noh, S. H. Im, J. H. Heo, T. N. Mandal, and S. Il Seok, Nano Lett. **13**, 1764 (2013).
[4] L. Etgar, P. Gao, Z. Xue, Q. Peng, A. K. Chandiran, B. Liu, M. K. Nazeeruddin, and M. Grätzel, J. Am. Chem. Soc. **134**, 17396 (2012).
[5] I. Chung, B. Lee, J. He, R. P. H. Chang, and M. G. Kanatzidis, Nature (London) **485**, 486 (2012).
[6] J. Qiu, Y. Qiu, K. Yan, M. Zhong, C. Mu, H. Yan, and S. Yang, Nanoscale **5**, 3245 (2013).
[7] O. Malinkiewicz, A. Yella, Y. H. Lee, G. M. Espallargas, M. Grätzel, M. K. Nazeeruddin, and H. J. Bolink, Nat. Photonics **8**, 128 (2013).
[8] M. Liu, M. B. Johnston, and H. J. Snaith, Nature (London) **501**, 395 (2013).
[9] D. Liu and T. L. Kelly, Nat. Photonics **8**, 133 (2013).
[10] W. A. Laban and L. Etgar, Energy Environ. Sci. **6**, 3249 (2013).
[11] J. H. Heo, S. H. Im, J. H. Noh, T. N. Mandal, C.-S. Lim, J. A. Chang, Y. H. Lee, H. Kim, A. Sarkar, M. K. Nazeeruddin, M. Grätzel, and S. Il Seok, Nat. Photonics **7**, 486 (2013).
[12] J. Burschka, N. Pellet, S.-J. Moon, R. Humphry-Baker, P. Gao, M. K. Nazeeruddin, and M. Grätzel, Nature (London) **499**, 316 (2013).
[13] J. M. Ball, M. M. Lee, A. Hey, and H. J. Snaith, Energy Environ. Sci. **6**, 1739 (2013).
[14] A. Abrusci, S. D. Stranks, P. Docampo, H.-L. Yip, A. K.-Y. Jen, and H. J. Snaith, Nano Lett. **13**, 3124 (2013).
[15] J. You, Z. Hong, Y. M. Yang, Q. Chen, M. Cai, T. Song, C. Chen, S. Lu, Y. Liu, H. Zhou, and Y. Yang, ACS Nano **8**, 1674 (2014).
[16] Y. Ogomi, A. Morita, S. Tsukamoto, T. Saitho, N. Fujikawa, Q. Shen, T. Toyoda, K. Yoshino, S. S. Pandey, T. Ma, and S. Hayase, J. Phys. Chem. Lett. **5**, 1004 (2014).
[17] P.-W. Liang, C.-Y. Liao, C.-C. Chueh, F. Zuo, S. T. Williams, X.-K. Xin, J. Lin, and A. K.-Y. Jen, Adv. Mater. **26**, 3748–3754 (2014).
[18] G. E. Eperon, V. M. Burlakov, A. Goriely, and H. J. Snaith, ACS Nano **8**, 591 (2014).
[19] Q. Chen, H. Zhou, Z. Hong, S. Luo, H.-S. Duan, H.-H. Wang, Y. Liu, G. Li, and Y. Yang, J. Am. Chem. Soc. **136**, 622 (2014).
[20] A. Dualeh, N. Tétreault, T. Moehl, P. Gao, M. K. Nazeeruddin, and M. Grätzel, Adv. Funct. Mater. **24**, 3250–3258 (2014).
[21] T. Leijtens, B. Lauber, G. E. Eperon, S. D. Stranks, and H. J. Snaith, J. Phys. Chem. Lett. **5**, 1096 (2014).
[22] M. Saliba, K. W. Tan, H. Sai, D. T. Moore, T. Scott, W. Zhang, L. A. Estroff, U. Wiesner, and H. J. Snaith, J. Phys. Chem. C (2014).
[23] K. W. Tan, D. T. Moore, M. Saliba, H. Sai, L. A. Estroff, T. Hanrath, H. J. Snaith, and U. Wiesner, ACS Nano **8**, 4730 (2014).
[24] G. E. Eperon, V. M. Burlakov, P. Docampo, A. Goriely, and H. J. Snaith, Adv. Funct. Mater. **24**, 151 (2014).
[25] Y. Zhao and K. Zhu, J. Phys. Chem. C **118**, 9412 (2014).
[26] E. Edri, S. Kirmayer, M. Kulbak, G. Hodes, and D. Cahen, J. Phys. Chem. Lett. **5**, 429 (2014).
[27] J.-Y. Jeng, K.-C. Chen, T.-Y. Chiang, P.-Y. Lin, T.-D. Tsai, Y.-C. Chang, T.-F. Guo, P. Chen, T.-C. Wen, and Y.-J. Hsu, Adv. Mater. **26**, 4107–4113 (2014).
[28] J.-H. Im, C.-R. Lee, J.-W. Lee, S.-W. Park, and N.-G. Park, Nanoscale **3**, 4088 (2011).
[29] D. H. Son, S. M. Hughes, Y. Yin, and A. P. Alivisatos, Science **306**, 1009 (2004).
[30] L. Li, N. Sun, Y. Huang, Y. Qin, N. Zhao, J. Gao, M. Li, H. Zhou, and L. Qi, Adv. Funct. Mater. **18**, 1194 (2008).
[31] H. Jeen, W. S. Choi, J. W. Freeland, H. Ohta, C. U. Jung, and H. N. Lee, Adv. Mater. **25**, 3651 (2013).
[32] K. Nakajima, Y. Oaki, and H. Imai, ChemPlusChem **78**, 1379 (2013).
[33] P. Wen, Y. Ishikawa, H. Itoh, and Q. Feng, J. Phys. Chem. C **113**, 20275 (2009).
[34] H. Uchiyama and H. Imai, Langmuir **24**, 9038 (2008).
[35] N. Kitazawa, Y. Watanabe, and Y. Nakamura, J. Mater. Sci. **37**, 3585 (2002).

[36] S. Colella, E. Mosconi, P. Fedeli, A. Listorti, F. Gazza, F. Orlandi, P. Ferro, T. Besagni, A. Rizzo, G. Calestani, G. Gigli, F. De Angelis, and R. Mosca, Chem. Mater. **25**, 4613 (2013).
[37] A. Poglitsch and D. Weber, J. Chem. Phys. **87**, 6373 (1987).
[38] See supplementary material at http://dx.doi.org/10.1063/1.4886275 for full experimental methods, 2D GIWAXS images, additional SEM micrographs, and FTIR spectra.
[39] M. Olszak-Humienik, Thermochim. Acta **378**, 107 (2001).
[40] O. Yamamuro, M. Oguni, T. Matsuo, and H. Suga, Thermochim. Acta **98**, 327 (1986).
[41] V. Roiati, E. Mosconi, A. Listorti, S. Colella, G. Gigli, and F. De Angelis, Nano Lett. **14**, 2168 (2014).